Electronic Supplementary Information

Anion and solvent controlled growth of crystalline and amorphous zinc(II) coordination polymers and a molecular complex

Claire Deville,[a] Henrik S. Jeppesen,[a] Vickie McKee,[b] and Nina Lock[c§*]

[a]Interdisciplinary Nanoscience Center (iNANO), Aarhus University, Gustav Wieds Vej 14, DK-8000 Aarhus C, Denmark

[b]Dept. of Physics, Chemistry and Pharmacy, University of Southern Denmark, Campusvej 55, DK-5230 Odense M, Denmark

[c]Carbon Dioxide Activation Center, Interdisciplinary Nanoscience Center (iNANO) and Dept. of Chemistry, Aarhus University, Gustav Wieds Vej 14, DK-8000 Aarhus C, Denmark

[§]Current address: Dept. of Biological and Chemical Engineering, Aarhus University, Aabogade 40, DK-8200 Aarhus N, Denmark

*corresponding author: nlock@bce.au.dk

1. Crystal structures at 100 K

*{[Zn(tph)(L)]·H_2O·3DMF}$_n$ (**1**·H_2O·3DMF)*

The structure of **1**·H_2O·3DMF was solved as a single enantiomer. The Flack parameter slightly deviates from zero and has a rather high uncertainty. This is essentially attributed to the Ag radiation. Solving the structure as an inversion twin did not provide any significant improvement. The BASF values obtained in that case are mentioned in the cif. The structure contains some solvent accessible voids.

The structural drawings presented here are based on 100 K single crystal diffraction data.

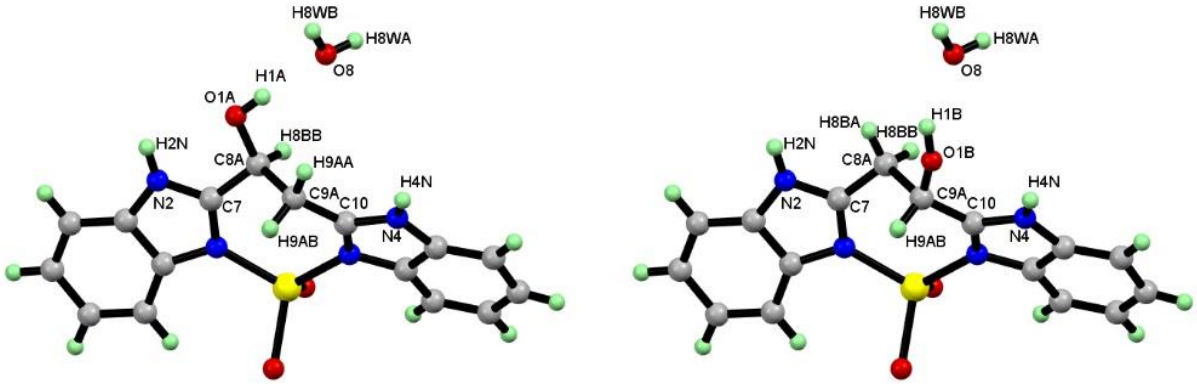

Fig. S1. Positional disorder of L in the crystal structure of **1**·H_2O·3DMF. The major component (60%) is displayed on the left, and the minor component (40%) on the right. In both cases, the hydrogen of the alcohol function forms a hydrogen bond with O8 (water molecule) as an acceptor.

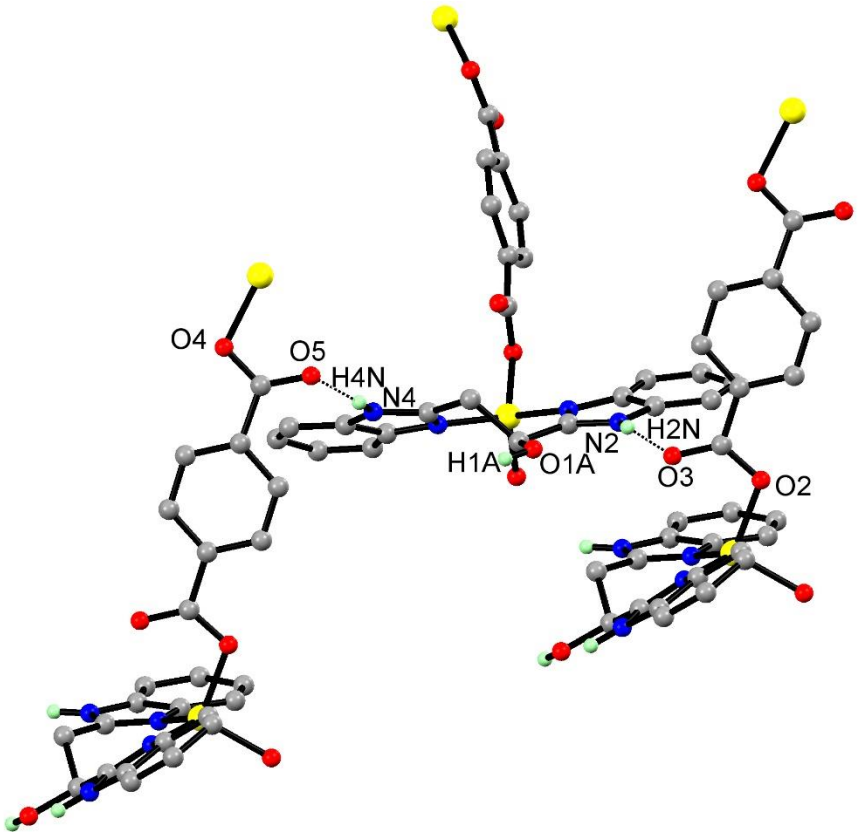

Fig. S2. Hydrogen bonds involving the NH functions of the benzimidazole rings (shown in dashed lines) in the crystal structure of **1**·H_2O·3DMF. The hydrogen atoms not involved in any hydrogen bonding are omitted for clarity.

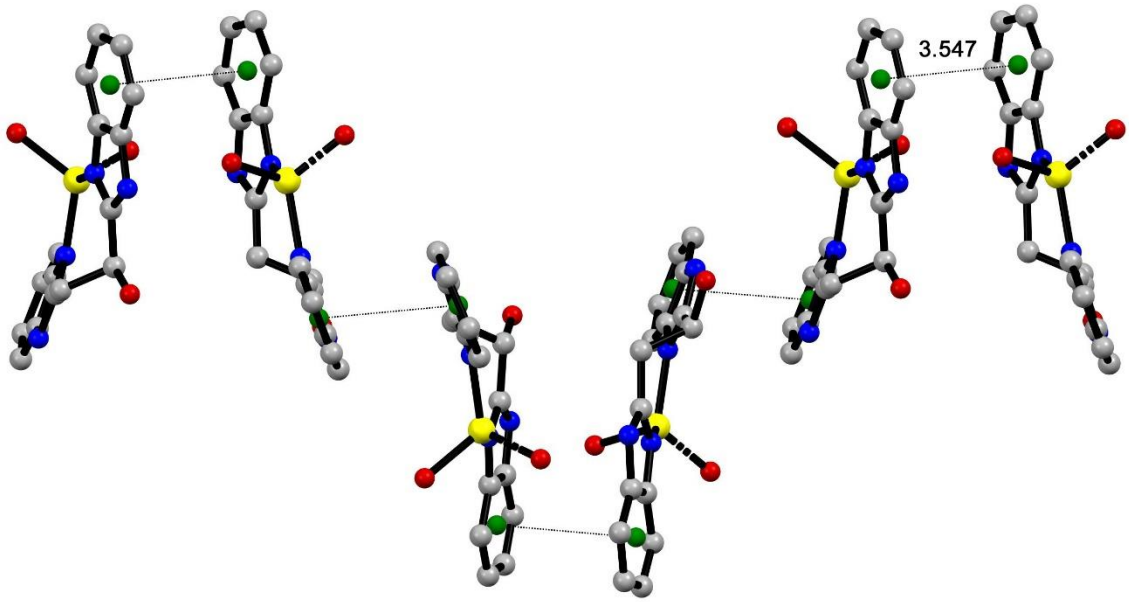

Fig. S3. π-stacking between the benzimidazole rings of neighbouring chains in the crystal structure of **1**·H_2O·3DMF. The centroid of the six-membered ring of the benzimidazole function is shown in green. The distance between two centroids is 3.547 Å and all the interactions are equivalent. The hydrogen atoms, solvent molecules and terephthalate linkers are not shown for clarity.

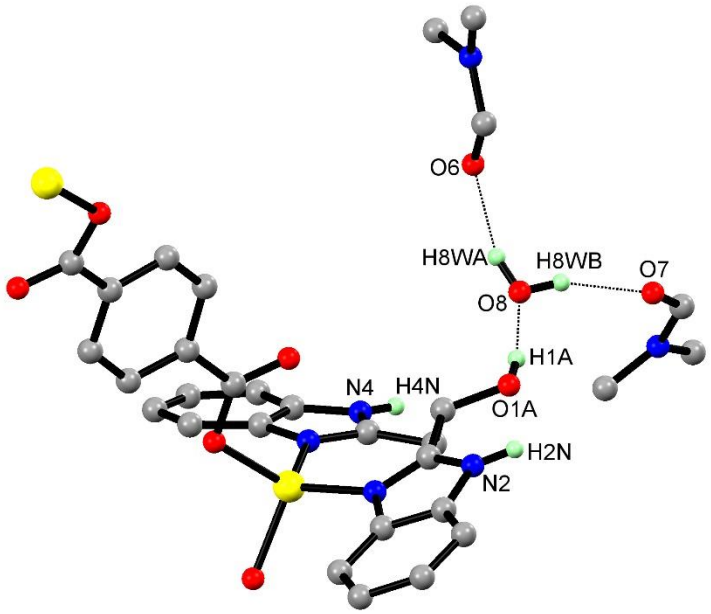

Fig. S4. Hydrogen bonding network involving the solvent molecules (shown in dashed lines) in the crystal structure of **1**·H_2O·3DMF. The hydrogen atoms not involved in any hydrogen bond have been omitted for clarity.

Table S1. Hydrogen bond geometry (Å, º) for {[Zn(tph)(L)]·H_2O·3DMF}$_n$ (**1**·H_2O·3DMF)

D—*H*···*A*	*D*—*H*	H···A	*D*···*A*	*D*—*H*···*A*
N2—H2N···O3iii	0.90 (3)	1.90 (5)	2.728 (7)	152 (8)
N4—H4N···O5iv	0.89 (3)	1.86 (4)	2.721 (7)	162 (8)
O8—H8WA···O6	0.85 (3)	1.90 (3)	2.711 (11)	159 (8)
O8—H8WB···O7	0.85 (3)	1.97 (3)	2.776 (10)	159 (9)
O1A—H1A···O8	0.84	1.86	2.687 (10)	169
O1B—H1B···O8	0.84	1.91	2.687 (16)	153

Symmetry codes: (iii) *y*, -*x*+1, *z*-1/4; (iv) *y*+1, -*x*+1, *z*-1/4.

Document origin: *publCIF* [Westrip, S. P. (2010). *J. Apply. Cryst.*, **43**, 920-925].

[Zn$_2$Cl$_2$(tph)(L)$_2$]·4DMF *(**2**·4DMF)*

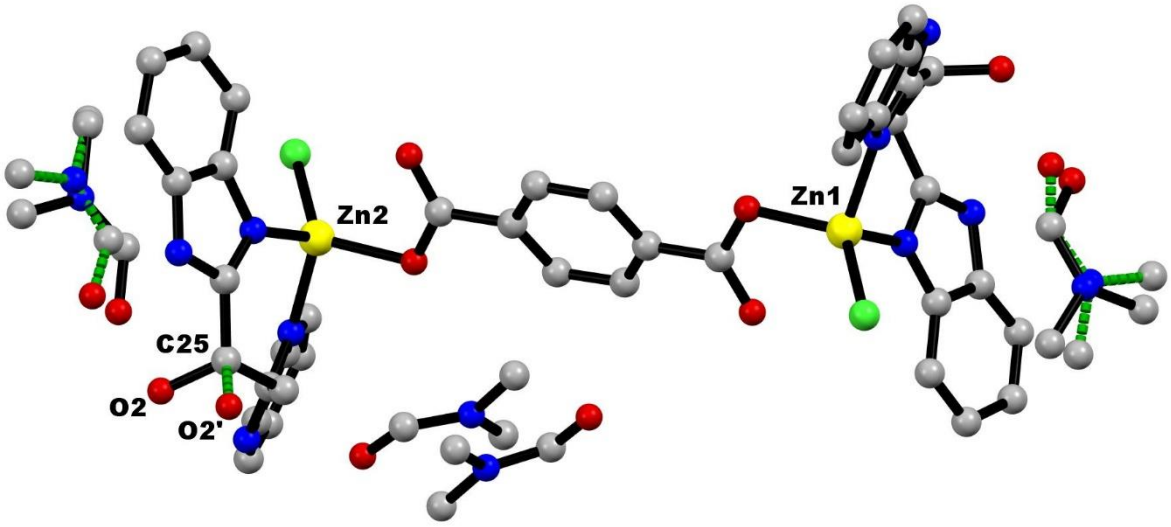

Fig. S5. Asymmetric unit in the crystal structure of **2**·4DMF showing the modelled disorder of two DMF molecules (second component with green bonds), as well as the alcohol function on the bisbenzimidazole ligand coordinated to Zn2 (the major component with a black bond, and the minor component with a green bond).

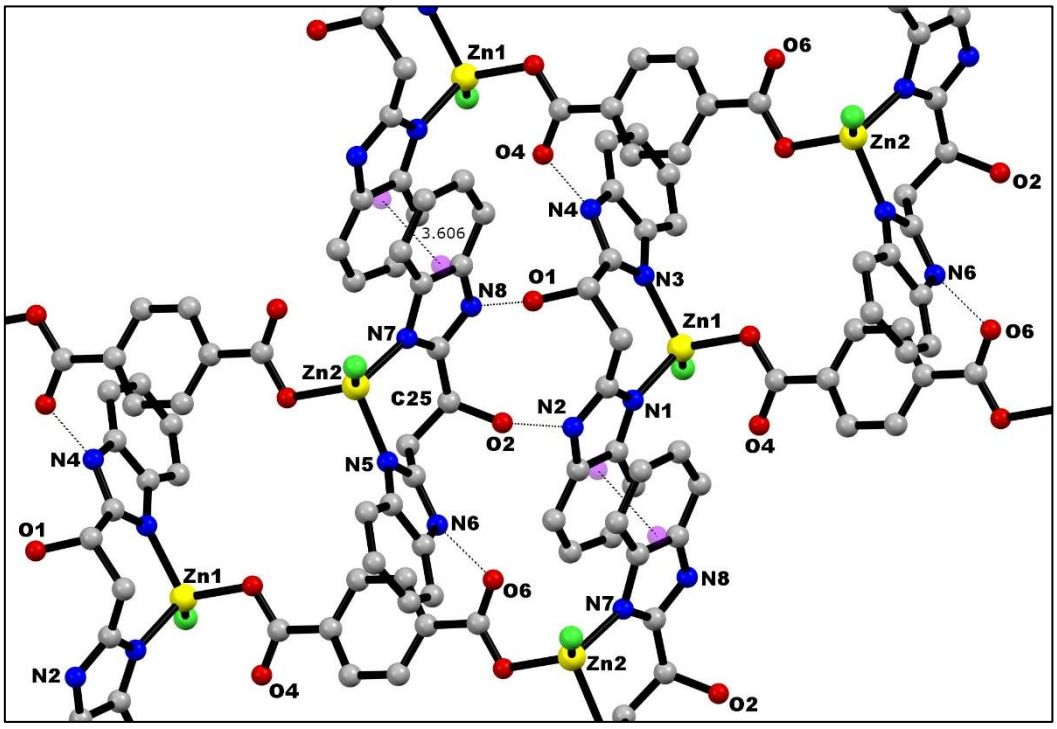

Fig. S6. Hydrogen bonding network and π-stacking between neighbouring molecules of **2** in the structure of **2**·4DMF. The hydrogen bonds are shown in dashed lines. The solvent molecules as well as the hydrogen atoms have been omitted for clarity. The π-stacking interaction has been measured between the centroids (purple spheres, 3.606 Å) of the two benzimidazole rings involved.

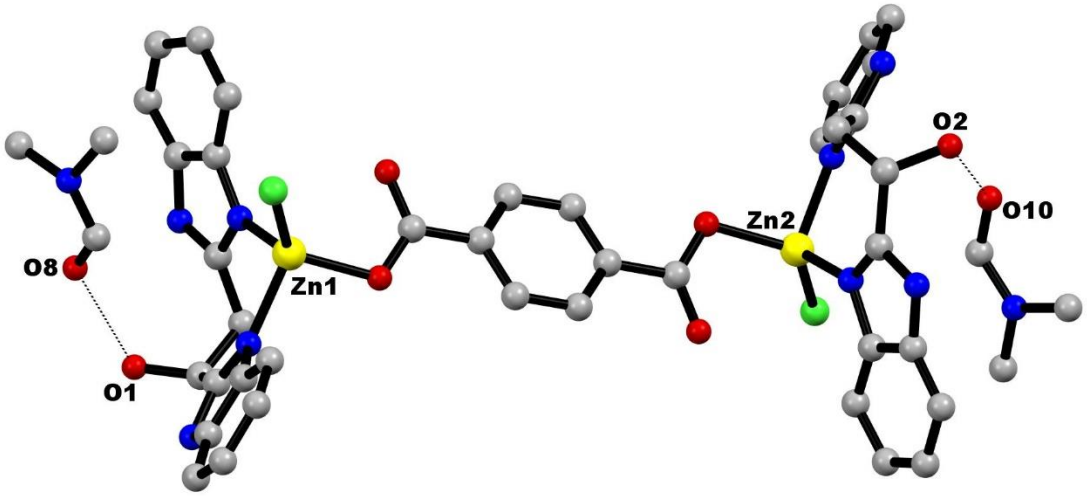

Fig. S7. Hydrogen bonding interaction between a molecule of **2** and neighbouring solvent molecules in the structure of **2**·4DMF. The hydrogen bonds are shown as dashed lines. The hydrogen atoms have been omitted for clarity.

Table S2. Hydrogen bond geometry (Å, º) for $[Zn_2Cl_2(tph)(L)_2]$·4DMF (**2**·4DMF)

D—H···A	*D—H*	H···A	*D···A*	*D—H···A*
O1—H1O···O8a	0.87	1.93	2.66 (3)	141
O2a—H2Oa···O10a	0.92	1.94	2.79 (3)	152
N2—H2N···O2ai	0.88	1.88	2.76 (3)	176
N4—H4N···O4ii	0.88	1.92	2.75 (2)	158
N6—H6N···O6iii	0.88	1.83	2.71 (2)	173
N8—H8···O1iv	0.88	1.98	2.84 (2)	166
O2′b—H2′b···O9	0.84	2.63	2.78 (4)	92

Symmetry codes: (i) *x*+1, *y*, *z*-1; (ii) *x*+1, *y*, *z*; (iii) *x*-1, *y*, *z*+1; (iv) *x*-1, *y*, *z*.

Document origin: *publCIF* [Westrip, S. P. (2010). *J. Apply. Cryst.*, **43**, 920-925].

2. Variable temperature single crystal diffraction

Data were collected on the same single crystal of **1**·H_2O·3DMF at 100-400 K in 50 K intervals. Full structure solution was obtained at 100 K, 150 K, 200 K, and 250 K, whereas the 300 K measurement only led to a poor structure solution. Due to weak diffraction at 350 K and 400 K only rough estimates of the unit cell were obtained at these temperatures. The reason for this was not investigated further, but might be caused by solvent rearrangement in the crystal. Therefore, only data in the range 100-250 K form basis for the investigation of the thermal relaxation of the linkers.

Table S3. Crystallographic data for **1**·H_2O·3DMF at 150 K, 200 K and 250 K (100 K summary in manuscript).

Compound	**1·H_2O·3DMF (150 K)**	**1·H_2O·3DMF (200 K)**	**1·H_2O·3DMF (250 K)**
Chemical formula	$C_{24}H_{18}N_4O_5Zn$ ·$(C_3H_7NO)_3$·H_2O	$C_{24}H_{18}N_4O_5Zn$ ·$(C_3H_7NO)_3$·H_2O	$C_{24}H_{18}N_4O_5Zn$ ·$(C_3H_7NO)_3$·H_2O
M_r (u)	745.10	745.10	745.10
λ (Å)	0.56086 Å	0.56086 Å	0.56086 Å
T (K)	150	200	250
Crystal system	Tetragonal	Tetragonal	Tetragonal
Space Group	$P4_1$	$P4_1$	$P4_1$
a (Å)	13.6439(7)	13.7346(12)	13.7729(8)
b (Å)	13.6439(7)	13.7346(12)	13.7729(8)
c (Å)	19.6066(10)	19.6084(17)	19.5804(12)
α (°)	90	90	90
β (°)	90	90	90
γ (°)	90	90	90
V (Å^3)	3649.9(4)	3698.9(7)	3714.3(5)
Z	4	4	4
ρ/(g/cm^3) (diffraction)	1.356	1.338	1.332
F(000)	1560	1560	1560
θ_{min}, θ_{max} (°)	1.178, 20.562	1.170/20.566	1.167/20.558
μ (mm^{-1})	0.39 (AgK_α)	0.39 (AgK_α)	0.380 (AgK_α)
Collected reflections	63305	70999	50711
Unique reflections (all)	7482	7604	7637
Unique reflections [$I \geq 2\sigma(I)$]	6612	6731	6778
Parameters/restraints	433/8	433/34	433/32
$R1$ (all data), $R1[I \geq 2\sigma(I)]$ (%)	5.82/5.04	5.10/4.26	4.48/3.76
Goodness-of-fit	1.071	1.094	1.068
$\Delta\rho$(max, min) (e/Å^3)	0.87/-0.40	0.56/-0.31	0.28/-0.27
Flack Parameter	0.048(6)	0.036(6)	0.028(6)

The positions of two DMF molecules and one water molecule were determined by structure solution. Moreover, remaining diffuse electron density was treated using the SQUEEZE[1] procedure which located a single void. The electron density for each dataset was ascribed to a

number of DMF molecules as presented in Table S4. All data were collected on the same crystal.

Table S4. SQUEEZE procedure output at different temperatures

***T* (K)**	**Squeezed e^- per cell**	**e^- per asymmetric unit**	**#(DMF)/asym. unit**
100	143	35.75	0.89
150	161	40.25	1.01
200	183	45.75	1.14
250	154	38.50	0.96

Table S5. Unit cell of **1**·H_2O·3DMF at variable temperatures. Note: the larger uncertainty on the values at 350 and 400 K is due to the very weak diffraction, and full data sets were not collected at these temperatures.

***T* (K)**	***a* (Å)**	***b* (Å)**	***c* (Å)**
100	13.6127(13)	13.6127(13)	19.6051(18)
150	13.6439(7)	13.6439(7)	19.6066(10)
200	13.7346(12)	13.7346(12)	19.6084(17)
250	13.7729(8)	13.7729(8)	19.5804(12)
300	13.9155(48)	13.9155(48)	19.5525(63)
350	14.16(50)	14.16(50)	19.6(8)
400	14.44(30)	14.44(30)	19.65(40)

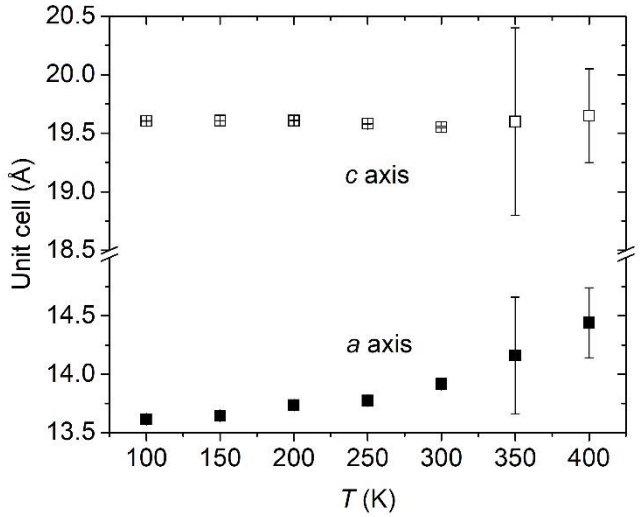

Fig. S8. Temperature dependent *a* = *b* axis (filled squares) and *c* axis (open squares) of **1**·H_2O·3DMF as determined by single crystal diffraction.

Table S6. Geometric parameters involving the Zn atom in the structure of **1**·H_2O·3DMF at different temperatures.

	100 K	150 K	200 K	250 K
Zn1—O4^{i}	1.965 (4)	1.966 (4)	1.963 (3)	1.962 (3)
Zn1—O2	1.970 (4)	1.972 (4)	1.969 (3)	1.962 (3)
Zn1—N3	1.974 (5)	1.967 (5)	1.973 (4)	1.976 (4)
Zn1—N1	1.990 (5)	1.983 (5)	1.983 (4)	1.985 (4)
O4^{i}—Zn1—O2	100.27 (17)	100.24 (16)	100.23 (14)	100.22 (11)
O4^{i}—Zn1—N3	110.5 (2)	110.59 (19)	110.65 (16)	110.63 (14)
O2—Zn1—N3	115.96 (19)	115.87 (18)	115.90 (16)	115.60 (14)
O4^{i}—Zn1—N1	115.44 (19)	115.12 (18)	115.06 (16)	115.07 (13)
O2—Zn1—N1	107.1 (2)	106.9 (2)	107.19 (17)	107.69 (14)
N3—Zn1—N1	107.6 (2)	108.1 (2)	107.88 (17)	107.71 (14)

3. Powder X-ray diffraction

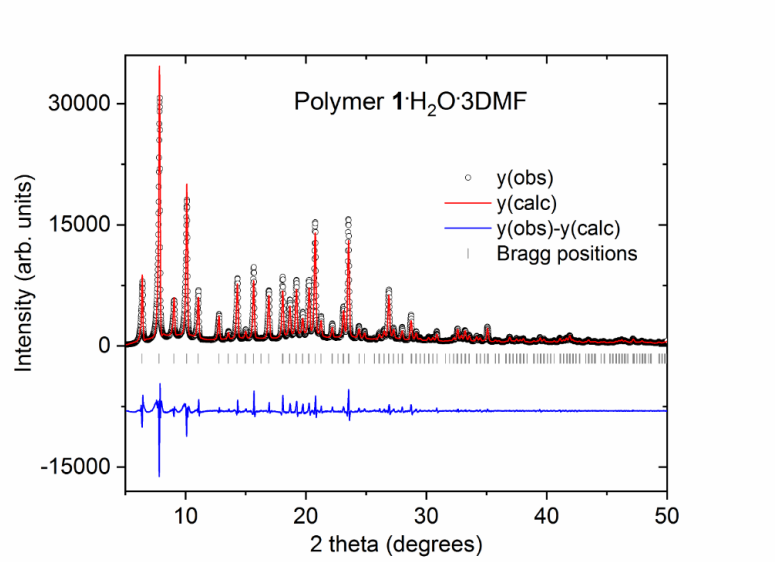

Fig. S9. Powder X-ray diffraction data of polymer **1**·H_2O·3DMF prepared from $Zn(ClO_4)_2$. The structural models obtained by single crystal diffraction was fitted to the data using the Le Bail method (data: open circles, model: red line, difference between data and model: blue line). Refined unit cell parameters (room temperature) for tetragonal **1**·H_2O·3DMF: $a = b$ = 13.8571(8) Å; c = 19.636(1) Å, R_p = 17.6%, R_{wp} = 19.3%. Refinement details: The background was described by linear interpolation of individual background points, and the profiles were described by a Thompson-Cox-Hastings pseudo-Voigt function with axial divergence asymmetry. Seven parameters were refined: *a* = *b*, *c*, *zero*. *W*, *Y*, *Asym1* and *Asym2*. *U* was fixed to a non-zero value.

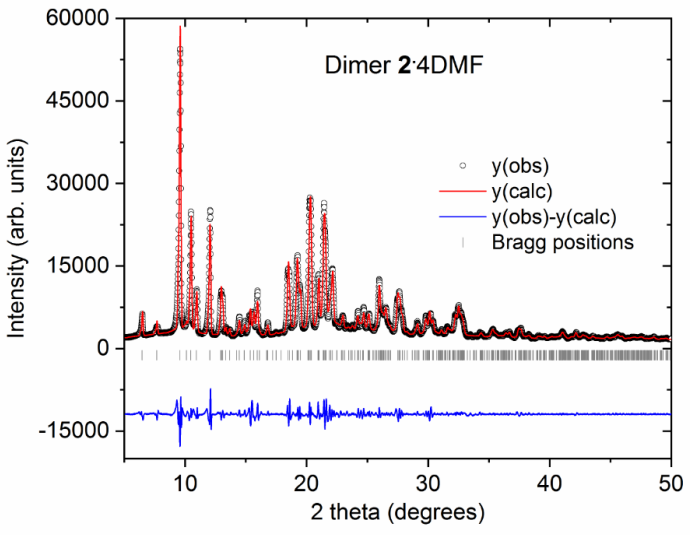

Fig. S10. Powder X-ray diffraction data of dimer **2**·4DMF synthesized from $ZnCl_2$. The structural model obtained by single crystal diffraction was fitted to the data using the Le Bail method (data: open circles, model: red line, difference between data and model: blue line). Refined unit cell parameters (room temperature) for triclinic **2**·4DMF: a = 8.9331(2) Å; b = 11.6272(4) Å; c = 13.9461(4) Å; α = 94.138(2)°; β = 100.380(3)°; γ = 95.267(2)°, R_p = 14.6%, R_{wp} = 16.4%. Refinement details: The background was described by linear interpolation of individual background points, and the profiles were described by a Thompson-Cox-Hastings pseudo-Voigt function with axial divergence asymmetry. Nine parameters were refined: *a*, *b*, *c*, *α*, *β*, *γ*, *zero*. *W* and *X*. *Asym1* and *Asym2* were fixed to non-zero values.

4. FT- IR Spectra

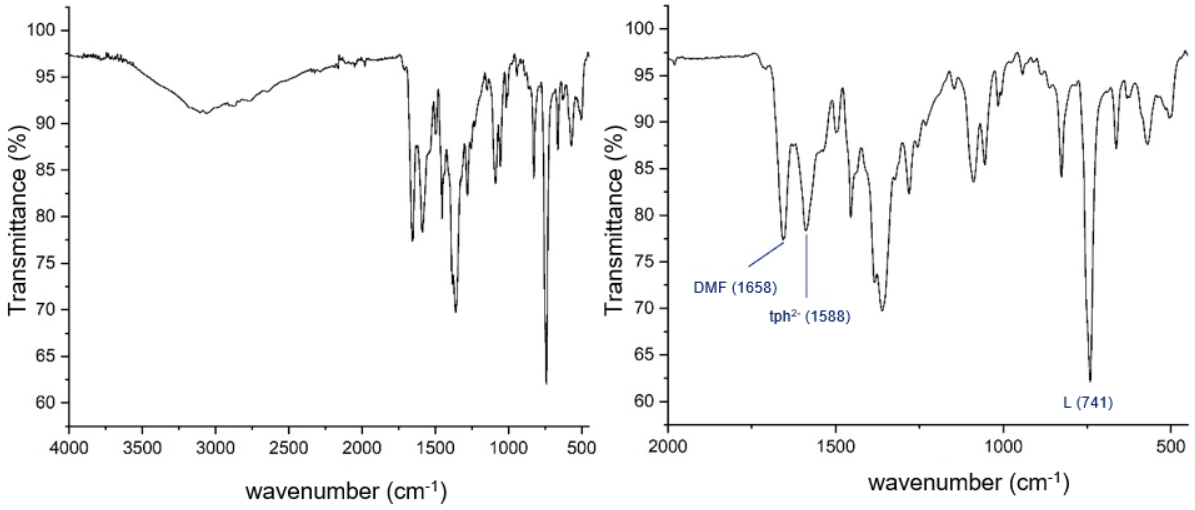

Fig. S11. FT-IR spectrum of compound **1**·H_2O·3DMF. IR data (cm^{-1}, intensity): 3068, bw; 1658, m; 1588, m; 1498, w; 1454, m; 1383, m; 1381, s; 1281, m; 1255, w; 1232, w; 1146, w; 1088, m; 1055, m; 1016, w; 942, w; 828, m; 741, s; 683, w; 630, w; 570, w; 505, w.

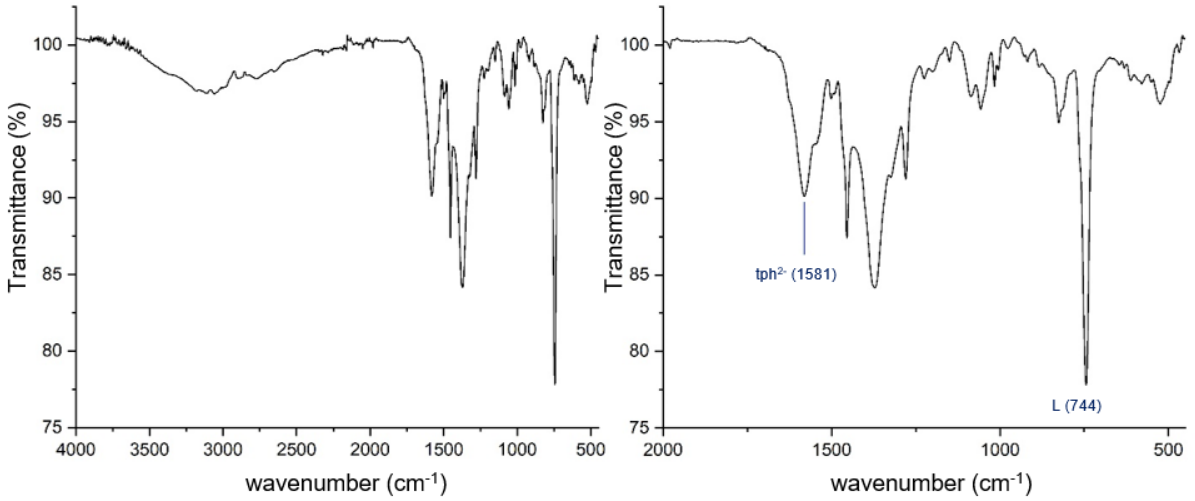

Fig. S12. FT-IR spectrum of compound **3**. IR data (cm^{-1}, intensity): 3059, bw; 1581, m; 1547, w; 1501, w; 1455, m; 1371, s, 1324, m; 1280, m; 1224, w; 1198, w; 1150, w; 1088, w; 1057, w; 1018, w; 978, w; 920, w; 826, w; 744, s; 612, w; 578, w; 524, w.

5. Scanning electron microscopy (SEM)

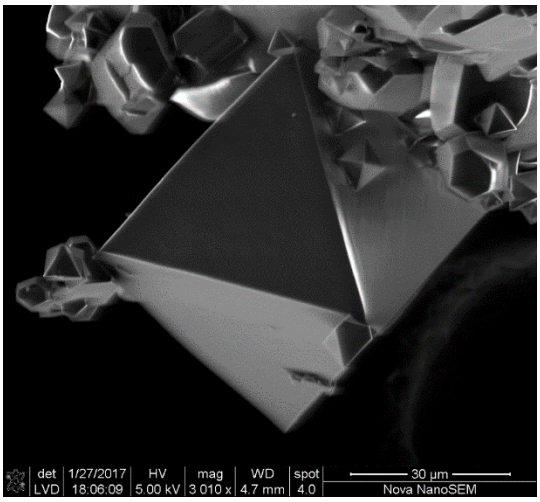

Fig. S13. SEM image of polymer **1**·H_2O·3DMF(as synthesized).

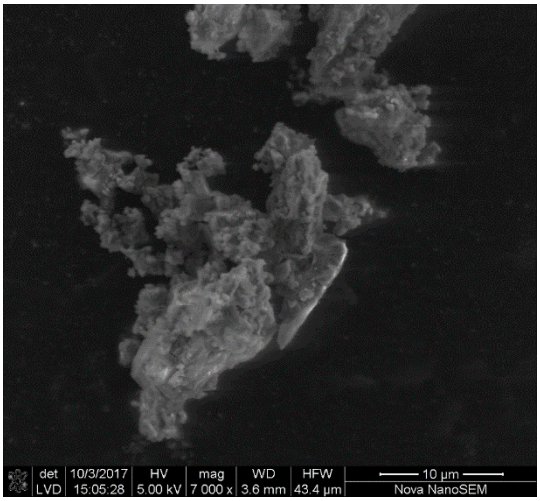

Fig. S14. SEM image of ground polymer **1**·H_2O·3DMF (sample used for the gas sorption analysis).

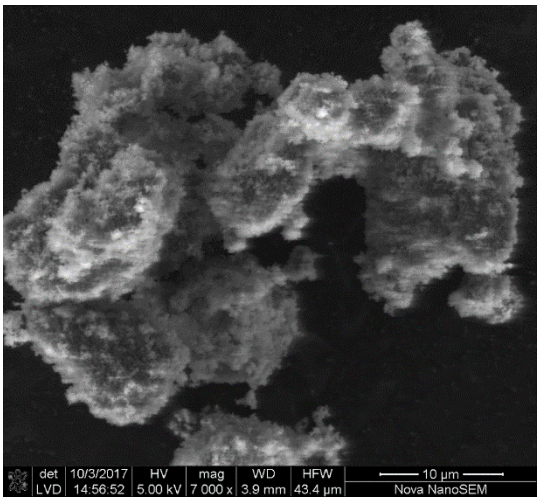

Fig. S15. SEM image of compound **3** used for the gas adsorption analysis.

Gas adsorption analysis

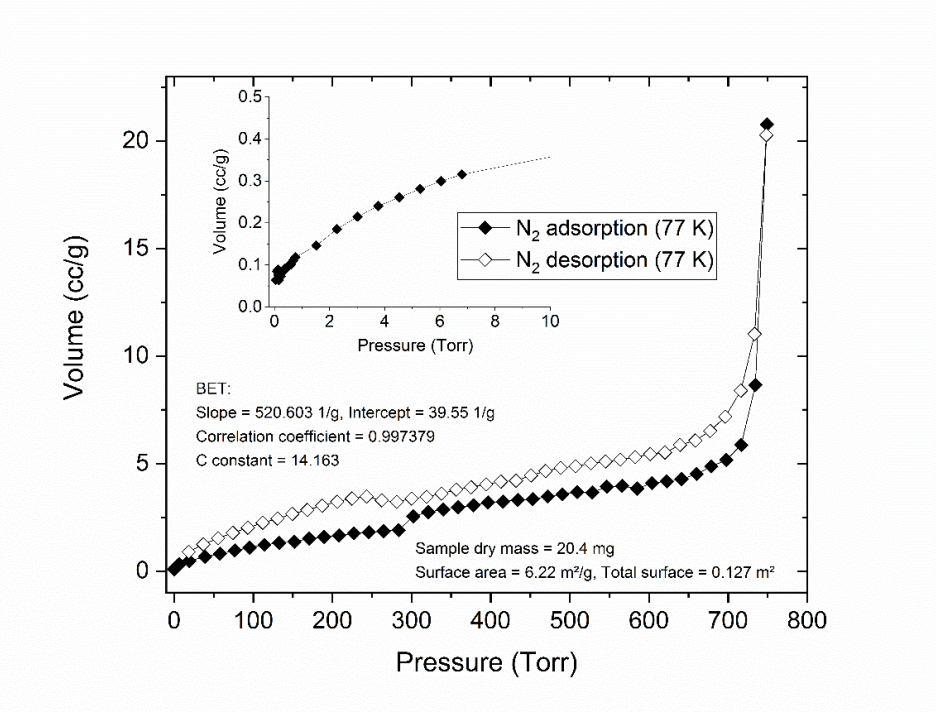

Fig. S16. Gas sorption analysis of **1**·H_2O·3DMF: N_2 adsorption/desorption at 77 K revealing type II isotherms corresponding to a non-porous compound. Adsorption and desorption curves are shown as closed and open diamonds. respectively. The insert shows the adsorption at low pressures. BET analysis gives a surface area of just 6.2 m^2/g.

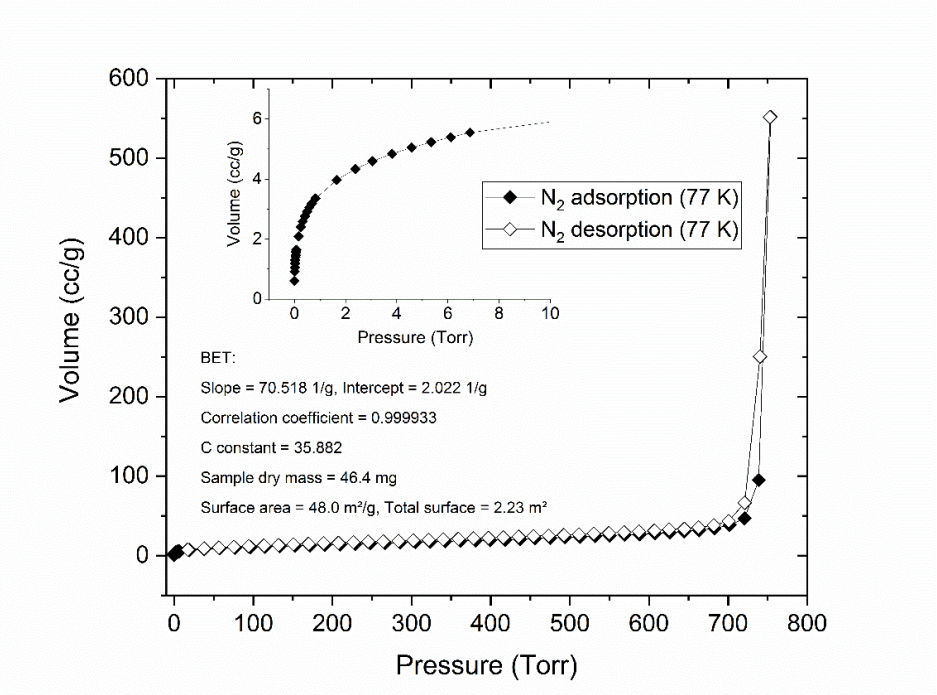

Fig. S17. Gas sorption analysis of compound **3**: N_2 adsorption (filled diamonds) and desorption (open diamonds) at 77 K revealing type II isotherms corresponding to a non-porous compound. The insert shows the adsorption at low pressures. BET analysis gives a surface area 48.0 m^2/g.

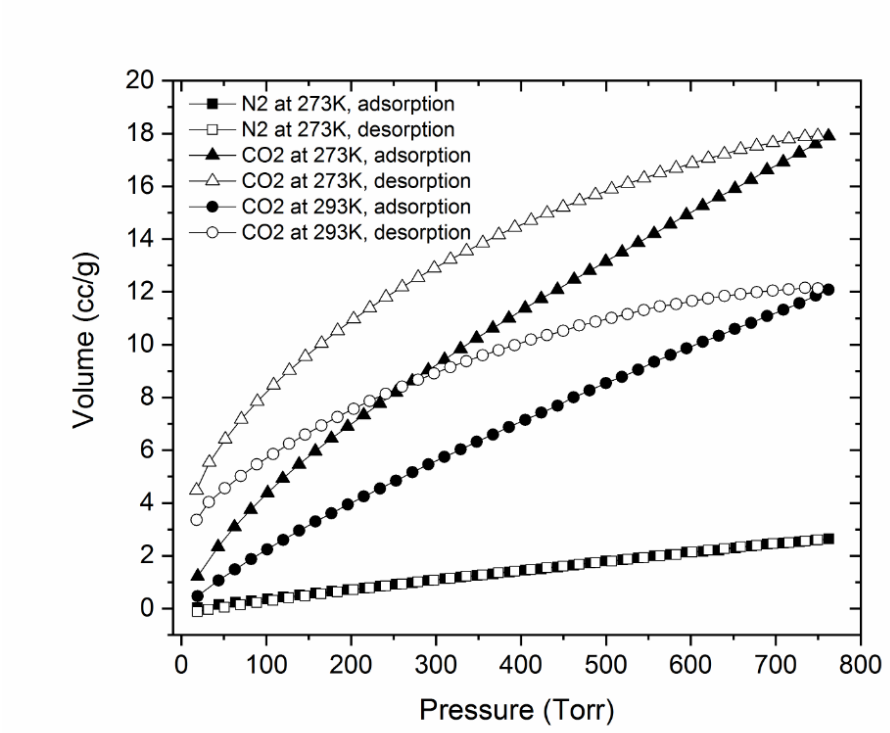

Fig. S18. Gas sorption analysis of compound **3**: N_2 adsorption (filled squares) and desorption (open squares) at 273 K, CO_2 adsorption (filled triangles) and desorption (open triangles) at 273 K, and CO_2 adsorption (filled circles) and desorption (open circles) at 293 K.

References

1. A. Spek, *Acta Crystallographica Section C*, 2015, **71**, 9-18.